Electric Power Systems Research 214 (2023) 108896

Contents lists available at ScienceDirect

Electric Power Systems Research

journal homepage: www.elsevier.com/locate/epsr

Lightning risk estimation and preventive control method for power distribution networks referring to the indeterminacy of wind power and photovoltaic

Yang Xu [a,*], Chong Tong [a], Min Xiang [a], Tao Wang [b], Jian Xu [b], Jianyong Zheng [c]

[a] State Grid Jiangsu Electric Power Co. Ltd. Suzhou Branch, Suzhou, China
[b] School of Electrical Engineering and Automation, Wuhan University, Wuhan, China
[c] School of Electrical Engineering, Southeast University, Nanjing, China

ARTICLE INFO

Keywords:
Power distribution network
Lightning risk estimation
Preventive control
Wind power
Photovoltaic

ABSTRACT

The power distribution networks are deeply influenced by the lightning weather. Such impact includes not only the load loss caused by the outage of the overhead lines due to direct and/or indirect lightning strikes, but also the output fluctuation of the wind power and photovoltaic (PV) connected to the network. Since lightning storms can be forecasted to some extent, it would be useful to establish a model for lightning risk estimation and preventive control of the distribution network, in order to cut the economic loss in extreme weather. In this paper, the scene analysis method is used to simulate the indeterminacy of the wind and PV output based on the lightning storm pre-warning, and the lightning risk and operating state of the distribution networks can be estimated. Referring to the results, lightning preventive strategy of distribution network can be formulated by network topology reconstruction and resource synergy.

1. Introduction

Lightning has always been a major natural factor endangering the safety of the power grid. More than 30% of power outages in the United States, and over half of grid disturbances and outages in Europe are caused by lightning each year. Especially in the distribution networks, hundreds of trip-outs can be caused in overhead distribution lines by a single time of lightning storm, and resulting in the power loss of large number of power consumers. Besides, due to the increase number of distributed wind turbine and photovoltaic connected to the network, the impact of lightning weather is becoming more remarkable, since the output power of the renewable energy will fluctuate drastically in such extreme weather, which may result in the power flow overload on the distribution lines and overvoltage on the critical network nodes.

Conventional measures for lightning protection of distribution networks includes the improvement of insulation level, installation of surge arresters and so on [1]. However, the power grid faults and load loss are still remarkable according to the operating experience, even if the network is well protected by one or several conventional measures.

The development of lightning detection and pre-warning technology in recent years provides a new idea so-called dynamic lightning protection (DLP) [2,3], which means to cut the economic loss of power network originated by lightning strikes by preventive control based on the forecast of lightning storms. Since DLP needs little adjustment on the existed power network and has decent effect on lightning protection, it has been regarded as the effective supplement to the conventional lightning protection measures, and one of the most promising research orientations in lightning protection area [4].

When DLP is supposed to be applicated in distribution networks, the model should be established to estimate the damage the lightning strikes will do to the grid, as well as the probable operation mode after the strikes, according to the announced lightning storm pre-warning. And then, feasible control strategy should be generated using the available resource in the regional grid, based on the anterior estimation results.

In this paper, the scene analysis method is used to simulate the indeterminacy of the wind and PV power output based on the lightning storm pre-warning, and the lightning risk and operating state of the distribution networks can be estimated. Referring to the results, lightning preventive strategy of distribution network can be formulated by network topology reconstruction and resource synergy.

* Corresponding author.
E-mail address: yang.xu@sgccsz.com (Y. Xu).

https://doi.org/10.1016/j.epsr.2022.108896
Received 10 July 2022; Received in revised form 26 September 2022; Accepted 11 October 2022
Available online 27 October 2022

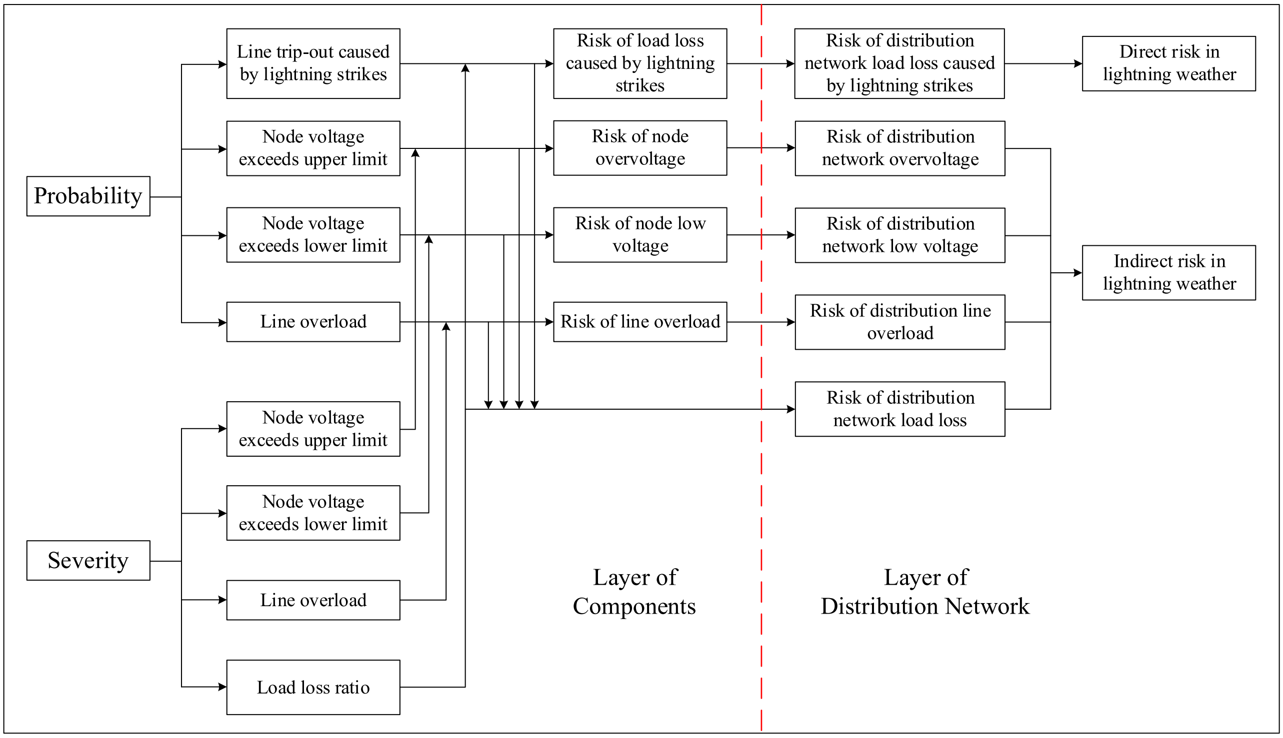

Fig. 1. The risk index system of distribution networks in lightning weather.

2. Risk estimation model

2.1. Modelling for the output of wind and PV power in lightning weather

The Copula function is used in this manuscript to analyze the relevance between the output of wind and PV power, which was firstly proposed by Sklar in 1959, and improved by Nelsen in 1998 [5,6]. In Sklar Theorem, if the marginal distribution functions of variables x_1, x_1, …, x_n are $F_1(x_1)$, $F_2(x_2)$, …, $F_n(x_n)$, then there will be a Copula function $C(F_1(x_1), F_2(x_2), \cdots, F_n(x_n))$ to build the joint distribution function $F(x_1, x_2, \cdots, x_n)$ for the anterior variables, namely

$$F(x_1, x_2, \cdots, x_n) = C(F_1(x_1), F_2(x_2), \cdots, F_n(x_n)). \tag{1}$$

Since the Copula function are of several types, it will be significant to select the most suitable type and corresponding parameters in such situation. In this manuscript, the empirical function and Euclidean distance are introduced as the basis of selection, for the simple operation and little impact from the marginal distribution function.

Moreover, in order to explicit the expression of the empirical Copula function, assume (x_i, y_i) as the samples of the two-dimension variable (X, Y), whose empirical distribution functions are $F_n(x)$ and $G_n(y)$, respectively, and the empirical Copula function $\widehat{C}_n(u,v)$ can be expressed as

$$\widehat{C}_n(u,v) = \frac{1}{n}\sum_{i=1}^{n} I_{[F_n(x_i)\le u]} I_{[G_n(y_i)\le v]}, \tag{2}$$

where the data range of variable u and v is $[0,1]$, and I is the indicative function,

$$I = \begin{cases} 1, & F_n(x_i) \le u \\ 0, & F_n(x_i) > u \end{cases}. \tag{3}$$

Assume the expression of Copula function is $C_n(u,v)$, calculate the Euclidean distance between $C_n(u,v)$ and $\widehat{C}_n(u,v)$ using the following formula

$$d_{gu} = \sqrt{\sum_{i=1}^{n} \left|\widehat{C}_n(u,v) - C_n(u,v)\right|^2}. \tag{4}$$

The smaller Euclidean distance, the higher fitting precision will be.

2.2. Scene extraction of the wind and PV power output in lightning weather

In order to obtain the representative scenes of the wind and PV power output in lightning weather, the probability function of the wind and PV power output in each period should be generated firstly using nonparametric kernel density estimation, based on the historical data in the past n days under the influence of lightning weather, as shown in Eq. (5).

$$\begin{cases} \widehat{f}_h^t(x^t) = \dfrac{1}{nh}\displaystyle\sum_{d=1}^{n} K\left(\dfrac{x^t - X_d^t}{h}\right) \\ \widehat{f}_h^t(y^t) = \dfrac{1}{nh}\displaystyle\sum_{d=1}^{n} K\left(\dfrac{y^t - Y_d^t}{h}\right) \end{cases} \tag{5}$$

In Eq. (5), t represents each period under the influence of lightning weather with duration of 15 min. x^t and y^t are the output of PV and wind power, respectively. $\widehat{f}_h^t(x^t)$ and $\widehat{f}_h^t(y^t)$ are the marginal probability density function of PV and wind power, respectively. X_d^t and Y_d^t are the output of PV and wind power in the t^{th} period of d^{th} day, respectively. $K(\cdot)$ is the Gaussian kernel density function shown in Eq. (6).

$$K\left(\frac{x^t - X_d^t}{h}\right) = \left(\frac{1}{\sqrt{2\pi}}\right)\exp\left[-\frac{\left(x^t - X_d^t\right)^2}{2h^2}\right] \tag{6}$$

In Eq. (6), h is the band width which can deeply affect on the accuracy of the kernel density estimation, and can be selected as

$$f_x(h) = E\left\{\int \left[\widehat{f}_h(x) - f_h(x)\right]^2 dx\right\}, \tag{7}$$

where $f_x(h)$ is the empirical distribution function, and the minimal value of $f_x(h)$ is the most suitable value of the band width h.

After the marginal probability density functions of PV and wind power are estimated with Eq. (5), the empirical Copula function $\widehat{C}_n(u,v)$ can be calculated with Eq. (2), and based on the Euclidean distance expressed in Eq. (4), the most suitable Copula function can be selected as the joint probability distribution function of PV and wind power. After that, inverse transform can be done on the cumulative distribution function the obtain the samples of the PV and wind power output.

Samples of the output in each period are treated as a scene. However, most of the scenes obtained in the last step are similar with each other, which will increase the computational cost. Hence, the K-means cluster method is introduced used to cut down the number of scenes. With this step, several representative output curves of PV and wind power will be derived, along with the probability of the corresponding scenes.

2.3. Estimation of the risk of power distribution network load loss in lightning weather

The risk of power distribution networks can be simplified as the product of the probability of the accident and its severity, which can be used to estimate the operation level of the system [7]. In this manuscript, the indeterminacy of the output of PV and wind power, along with the trip out of the distribution lines in lightning weather, are taken into account.

2.3.1. Risk level of distribution networks

The risk index system of distribution networks in lightning weather can be established based on the spatial composability of the risks, as shown in Fig. 1, which can be divided into two aspects, namely probability and severity. The index in the figure can be described as follows:

(1) *Risk of node overvoltage*

This index is introduced to reflect the risk that the node voltage exceeds the upper limit during operation. If the normal fluctuation range of the node voltage are limited between 0.95 to 1.05 p.u., the probability and risk of node overvoltage can be expressed as

$$Pr_i^{vh} = \sum_{s\in\Omega} Pr_{\mathrm{SC}} B_{i,s}^{vh}\left(V_{i,s}\right), \quad \forall i \tag{8}$$

$$R_i^{vh} = \sum_{s\in\Omega} Pr_{\mathrm{SC},s} B_{i,s}^{vh}\left(V_{i,s}\right) Sev^{vh}\left(V_{i,s}\right), \quad \forall i \tag{9}$$

$$Sev^{vh}\left(V_{i,s}\right) = \frac{e^{V_{i,s}-V_{\max}} - 1}{e-1}, \tag{10}$$

where Pr_i^{vh} represents the probability of overvoltage on Node i. $Pr_{\mathrm{SC},s}$ is the occurrence probability of Scene s. Ω is the set of the scenes of PV and wind power output. $B_{i,s}^{vh}$ is a Boolean quantity which equals to 1 if overvoltage appeared in Scene s, and otherwise, equals to 0. R_i^{vh} is the risk of overvoltage on Node i. Sev^{vh} is the severity of node overvoltage. $V_{i,s}$ is the per-unit value of the voltage on Node i in Scene s. $V_{\max}$ is the per-unit value of the maximum permissible voltage on Node i.

(2) *Risk of node low voltage*

This index is introduced to reflect the risk that the node voltage fell below the permissible value, which is usually 0.95 p.u.. The expression of the index is similar to Eq. (8) and (9), except for the expression of the severity of the risk, which can be expressed as

$$Sev^{vl}\left(V_{i,s}\right) = \frac{e^{V_{\min}-V_{i,s}} - 1}{e-1}. \tag{11}$$

The meanings of the variables are similar to those in the last index.

(3) *Risk of line overload*

The expression of the index is also similar to Eq. (8) and (9), except for the expression of the severity of the risk, which can be expressed as

$$Sev^{p}\left(P_{j,t,s}\right) = \frac{P_{j,t,s} - P_{j,\max}}{P_{j,\max}}, \tag{12}$$

where $P_{j,t,s}$ is the power on branch j at Time t in Scene s, and the unit is kW. The other variables are similar to those above.

(4) *Risk of load loss caused by lightning strikes*

Load loss is the direct harm of line trip-out. In order to describe such impact, the severity of the line trip-out caused by lightning strikes can be defined as

$$Pr_j^{l} = \sum_{s\in\Omega} Pr_{\mathrm{SC},s} Pr_{\mathrm{LST},s} B_{j,s}^{l}\left(P_{j,s}^{l}\right) \forall j \tag{13}$$

$$R_j^{l} = \sum_{s\in\Omega} Pr_{\mathrm{SC},s} Pr_{\mathrm{LST},s} B_{j,s}^{l}\left(P_{j,s}^{l}\right) Sev^{l}\left(P_{j,t,s}^{l}\right) \forall j \tag{14}$$

$$Sev^{l}\left(P_{j,t,s}^{l}\right) = \frac{P_{j,t,s}^{l}}{P_{j,t}}, \tag{15}$$

where $P_{j,t}$ is the active power of all the load in the distribution network before trip-out.

(5) *Risk of overvoltage, low voltage and over load*

This index is defined as the summary of the risk value of all the nodes in the network, and can be expressed as

$$R_{sys}^{vh} = \sum_{i=1}^{N_b} R_i^{vh}, \tag{16}$$

where R_{sys}^{vh} is the risk of distribution network overvoltage, and N_b is the number of the nodes in the network. Similarly, low voltage and over load risk of distribution network can be defined using the same format with different subscripts or superscripts.

(6) *Risk of load loss*

This index is defined to estimate the power loss of distribution networks due to the lightning strikes. As some indirect factors can result in the power loss, it is necessary to figure out the relationship among power loss, node voltage and branch power. In this manuscript, the criterion proposed in [8] is introduced to estimate the power loss due to the fluctuation of node voltage and branch power, namely when the node voltage falls below 0.6 p.u. or exceeds 1.2 p.u., or the branch power flow is 13.6% higher than the upper limit, all the loads connected to the node or the branch will be cut off. The relationship of system severity, node power loss and branch power loss can be expressed as

$$P_{load}^{vh} = \begin{cases} \frac{100}{9.4} Sev^{vh}, & Sev^{vh} \le 0.094 \\ 1, & Sev^{vh} > 0.094 \end{cases}, \tag{17}$$

$$P_{load}^{vl} = \begin{cases} \frac{100}{24.4} Sev^{vl}, & Sev^{vl} \le 0.244 \\ 1, & Sev^{vl} > 0.244 \end{cases}, \tag{18}$$

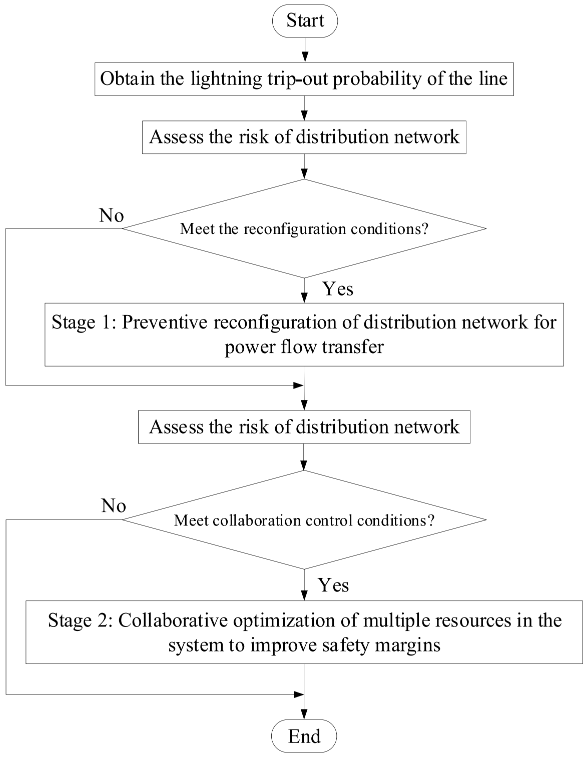

Fig. 2. Overall flow of the active lightning protection of distribution networks.

$$P^{p}_{load} = \begin{cases} \frac{100}{13.6} Sev^{p}, & Sev^{p} \le 0.136 \\ 1, & Sev^{p} > 0.136 \end{cases}, \tag{19}$$

where P^{vh}_{load}, P^{vl}_{load}, P^{p}_{load} are the percentage of power loss caused by overvoltage on the node, low voltage on the node and over load on the branch, respectively. V_i is the voltage on Node i. $V_{\max}$ and $V_{\min}$ are the upper and lower limit of the node voltage, respectively. P_j is the power on Branch i. $P_{j,\max}$ is the upper limit of the power on the branch. The risk of load loss due to overvoltage, power flow off-limit and lightning-caused trip out can be expressed as

$$R^{vh}_{load} = \sum_{i=1}^{N_b} \sum_{s\in\Omega} Pr_{SC,s} B^{vh}_{i,s}(V_{i,s}) P^{vh}_{load}, \ \forall i, \tag{20}$$

$$R^{vl}_{load} = \sum_{i=1}^{N_b} \sum_{s\in\Omega} Pr_{SC,s} B^{vl}_{i,s}(V_{i,s}) P^{vl}_{load}, \ \forall i, \tag{21}$$

$$R^{p}_{load} = \sum_{i=1}^{N_l} \sum_{s\in\Omega} Pr_{SC,s} B_{j,s}(P_{j,s}) P^{p}_{load}, \ \forall j, \tag{22}$$

$$R^{l}_{load} = \sum_{i=1}^{N_l} \sum_{s\in\Omega} Pr_{SC,s} Pr_{LST,s} B^{l}_{j,s}\left(P^{l}_{j,s}\right) P^{l}_{load}, \ \forall j. \tag{23}$$

Then the overall risk of load loss of the distribution network can be calculated as

$$R^{load1}_{sys} = \max\left\{R^{vh}_{load}, R^{vl}_{load}, R^{p}_{load}\right\}, \tag{24}$$

$$R^{load2}_{sys} = R^{l}_{load}. \tag{25}$$

where R^{load1}_{sys} is the overall risk of load loss due to overvoltage and power flow off-limit, and R^{load2}_{sys} is the risk of load loss due to lightning-caused trip out.

(7) Composite risk of the distribution network

The composite risk of the distribution network during the evaluation period can be defined as

$$CRI_1 = w_1 R^{vh}_{sys} + w_2 R^{vl}_{sys} + w_3 R^{p}_{sys} + w_4 R^{load1}_{sys}, \tag{26}$$

$$CRI_2 = R^{load2}_{sys}, \tag{27}$$

$$CRI = CRI_1 + CRI_2 \tag{28}$$

where CRI_1 is the composite risk due to overvoltage and power flow off-limit. w_1, w_2, w_3 and w_4 are the weight coefficients. CRI_2 is the composite risk due to lightning-caused trip out, and CRI is the composite risk of the distribution network.

2.3.2. Power flow calculation of the distribution network considering the load loss due to lightning-caused trip out

Due to the uncertainty of the wind and PV power output in lightning weather and the probable trip out of the lines, the smooth operation of the network might be interrupt. In such situation, the power flow optimization algorithm will be introduced to estimate the load loss caused by the lightning strikes, in order to minimize load loss under the constraints [9].

The conventional power flow optimization model is nonlinear, and in this manuscript, transformation will be realized on the conventional model using second order cone relaxation (SOCR). The target function in this model is the minimality of the load loss, which can be described as

$$\min \sum_{t}^{T} \left[a \times f\left(r, x, P_t, Q_t, \widetilde{V}_t, \widetilde{I}_t\right) + b \times \sum_{i}^{N_b} \Delta P_{L,i,t} \right], \tag{29}$$

where

$$f = \sum_{n=1}^{n_b} \widetilde{I}_{ij,t} r_{ij} = \sum_{n=1}^{n_b} \frac{\widetilde{V}_{j,t} - \widetilde{V}_{i,t} + 2\left(P_{ij,t} r_{ij} + Q_{ij,t} x_{ij}\right)}{\left(r^2_{ij} + x^2_{ij}\right)} r_{ij}, \tag{30}$$

r_{ij} and x_{ij} are the resistance and reactance of branch ij, respectively. $\widetilde{I}_{ij,t}$ is the square of the current on branch ij at time t. $P_{ij,t}$ and $Q_{ij,t}$ are the active and reactive power on branch ij at time t, respectively. $\widetilde{V}_{i,t}$ is the square of the voltage on node i at time t. $\Delta P_{L,i,t}$ is the load loss on node i at time t. N_b is the number of the nodes, and a, b are the corresponding weight coefficients.

The condition that the distribution network can keep operating smoothly after lightning-caused trip out is that some constraints are satisfied. Such constraints are usually about branch current, node voltage, load loss, node power balance, branch terminal voltage, energy storage devices, static VAR compensation (SVC), renewable energy output, and second order cone constraints, which can also be found in some previous researches [10].

3. Loss preventive model

Lightning-caused trip-out can result in large load loss in the distribution network, which can be divided in two sorts, namely the direct load loss and indirect load loss. The direct load loss refers to the loads which connected to the trip-out line and lost power supply immediately when accident took place, and the indirect load loss refers to the loads which was actively or passively cut off due to the subsequent system oscillation or power shortage caused by the trip-out. In order to reduce the load loss in such situation, backup power supply can be set up near the main line. However, in most of the time, no lightning can be detected even in the lightning-prone areas, making it not economical to install too many backup power sources.

A more promising measure for lightning protection in distribution networks is to implement preventive controls based on the risk estimation model before the lightning accident happens, by network topology refactoring, resource collaboration, branch power flow risk penalty, and so on [11].

In this sector, considering the different characteristics of direct and indirect load loss, the active protection of lightning in the distribution network will be divided into two stages, and the resources in the network will be fully invoked. The flowchart of the active protection for distribution networks is shown Fig. 2, namely to preventively reconfigure the network for power flow transfer once the lightning risk is accessed, and afterwards, to collaboratively optimize the multiple resources in the system to improve safety margins. Besides, considering the operating economy, such control measures will be implemented only when the risk level is above yellow alert.

3.1. Active prevention of lightning-caused direct load loss based on network reconstruction

The first stage is mainly about the topological reconstruction of the system. As lightning-caused trip-out usually results in heavy losses to the power grid, the existing contact switch will be used to reconstruct the network, and decision will be made according to the lightning threat area, the original network frame, and the load distribution of each period.

Since too much switching operations will not only reduce the service life of the switches, but also affect the stability of the distribution network, the number of topology reconstructions should be minimized based on the load loss and line status fluctuation in each period. For instance, if the status of the lines threatened by the lightning changes *N* times in the evaluation period, N times of reconstructions will be carried out based on the load distribution at the time the maximum load loss appeared.

3.1.1. Target function

Set $\widetilde{I}_{ij} = I_{ij}^2$ and $\widetilde{V}_i = V_i^2$, and SOCR transformation will be made on the conventional power flow optimization model. The target function will be set as

$$\min \sum_{t=1}^{T} \sum_{i=1}^{n_i} \left| \widetilde{V}_{i,t} - 1 \right|, \tag{31}$$

namely the maximization of the voltage security margin, ensuring the power system has the capacity to accommodate the fluctuation of wind and PV power output, and reduce the risk of overvoltage in the system. In this function, $\widetilde{V}_{i,t}$ is the square of the voltage on node *i* at time *t*. n_i is the number of the nodes, and *T* is the toal time of the evaluation period.

3.1.2. Constraints

When the distribution network is under reconstruction, several constraints should be satisfied as follows [12]:

(1) Constraints about nodes and branches

This sort of constraints is about node power balance, node voltage, branch current, and SOC constrains, which can be expressed as

$$\begin{cases} p_{j,t} = \sum_{k \in \delta(j)} P_{jk,t} - \sum_{i \in \pi(j)} \left(P_{ij,t} - \widetilde{I}_{ij,t} r_{ij} \right) + g_j \widetilde{V}_{j,t},\ j \in n_b \\ q_{j,t} = \sum_{k \in \delta(j)} Q_{jk,t} - \sum_{i \in \pi(j)} \left(Q_{ij,t} - \widetilde{I}_{ij,t} x_{ij} \right) + b_j \widetilde{V}_{j,t},\ j \in n_b \end{cases}, \tag{32}$$

$$\widetilde{V}_{j,t} = \widetilde{V}_{i,t} - 2\left(P_{ij,t} r_{ij} + Q_{ij,t} x_{ij}\right) + \widetilde{I}_{ij,t}\left(r_{ij}^2 + x_{ij}^2\right),\ \ ij \in n_l. \tag{33}$$

$$\left\| \begin{matrix} 2P_{ij,t} \\ 2Q_{ij,t} \\ \widetilde{I}_{ij,t} - \widetilde{V}_{j,t} \end{matrix} \right\|_2 \le \widetilde{I}_{ij,t} + \widetilde{V}_{j,t},\quad ij \in n_l \tag{34}$$

$$\begin{cases} I_{ij,\min}^2 \le \widetilde{I}_{ij,t} \le I_{ij,\max}^2,\quad ij \in n_l \\ V_{j,\min}^2 \le \widetilde{V}_{j,t} \le V_{j,\max}^2,\quad j \in n_b \end{cases} \tag{35}$$

where n_l is the set of the branches in the distribution network, and the other parameters are similar with that in Eq. (30).

(2) Constraints about network connectivity

While doing preventive reconstruction to the distribution network, the network connectivity should also be considered. For arbitrary node *i*,

$$a_j = 1,\quad \exists\ l_{i,0},\quad \forall j \in l_{i,0} \tag{36}$$

where $a_j = 1$ represents that branch *j* is closed. $l_{i,0}$ is the set of the branches which connects Node *i* with the source node of the network.

Besides, an assumption should be made in such situation that when the line under lightning threaten is disconnected, no circuit is existed in the network, namely

$$H = G + 1 \tag{37}$$

where H and G are the number of the nodes and branches in the network, respectively.

3.2. Active prevention of indirect load loss based on cooperative control of power source and load

The aim of this stage is to optimize the operation status of the distribution network, in order to minimize the impact of the fluctuation of wind and PV power output, and reduce the risk of voltage off-limit.

3.2.1. Target function

The security of operation of distribution network is the critical factor which should be considered in lightning weather. Hence, the target function should be set to reduce the overvoltage and load loss caused by the fluctuation of wind and PV power output, and meanwhile minimize the cost of preventive control. Detailed function can be expressed as

$$\min f = \min[\alpha f_1 + \beta f_2 + \gamma f_3], \tag{38}$$

where

$$f_1 = \sum_{t=1}^{T} \sum_{b=1}^{n_b} \frac{\widetilde{V}_{j,t} - \widetilde{V}_{i,t} + 2\left(P_{ij,t} r_{ij} + Q_{ij,t} x_{ij}\right)}{\left(r_{ij}^2 + x_{ij}^2\right)} r_{ij}, \tag{39}$$

$$f_2 = \sum_{t=1}^{T} \left(\sum_{i=1}^{n_b} \mu_i \left| \widetilde{V}_{i,t} - 1 \right| + \sum_{l=1}^{n_l} \mu_l U_{1,t} \left(\widetilde{I}_{l,t} - 0.4356 \widetilde{I}_{l,\max} \right) \right), \tag{40}$$

$$f_3 = \sum_{t=1}^{T} \sum_{b=1}^{n_b} \tau_b \left(P_{b,t}^{IL} + P_{b,t}^{TSL} \right). \tag{41}$$

μ_b and μ_l are the penalty coefficient for voltage excursion and orange alert, respectively. $U_{1,t}$ is a Boolean quantity, when $\widetilde{I}_{l,t} > 0.4356 \widetilde{I}_{l,\max}$, $U_{1,t} = 1$, otherwise, $U_{1,t} = 0$. τ_b is the cost coefficient of demand response on the load side. n_b is the number of the nodes with controllable loads. $P_{b,t}^{IL}$ and $P_{b,t}^{TSL}$ are the power of the interruptible load and load with time shift on node *b* at time *t*, respectively. α, β and γ are the weight coefficient. Other parameters are similar with that in Eq. (30).

3.2.2. Constraints

Except for the constraints in the last stage, constraints about load characteristics should be considered in this stage, which includes time shift and interruptible characteristics. The time shift characteristics represent the power of the load can be adjusted according to the demand while the total load demand remains unchanged. The constraints can be described as

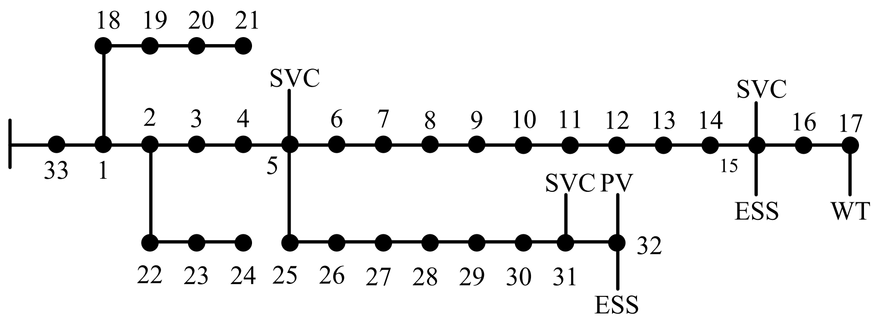

Fig. 3. The topology of IEEE 33 nodes power distribution system.

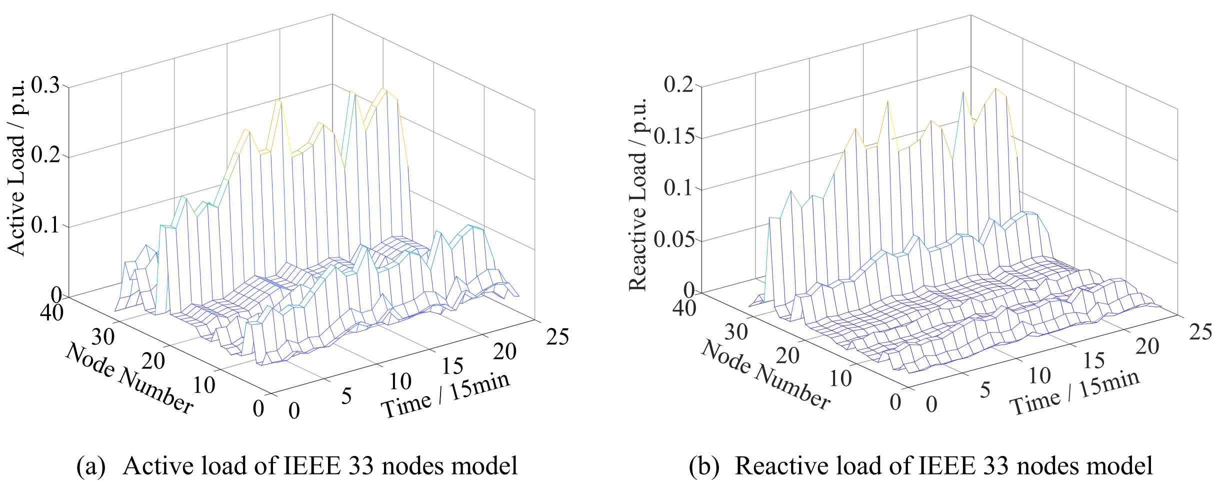

Fig. 4. Load on the nodes.

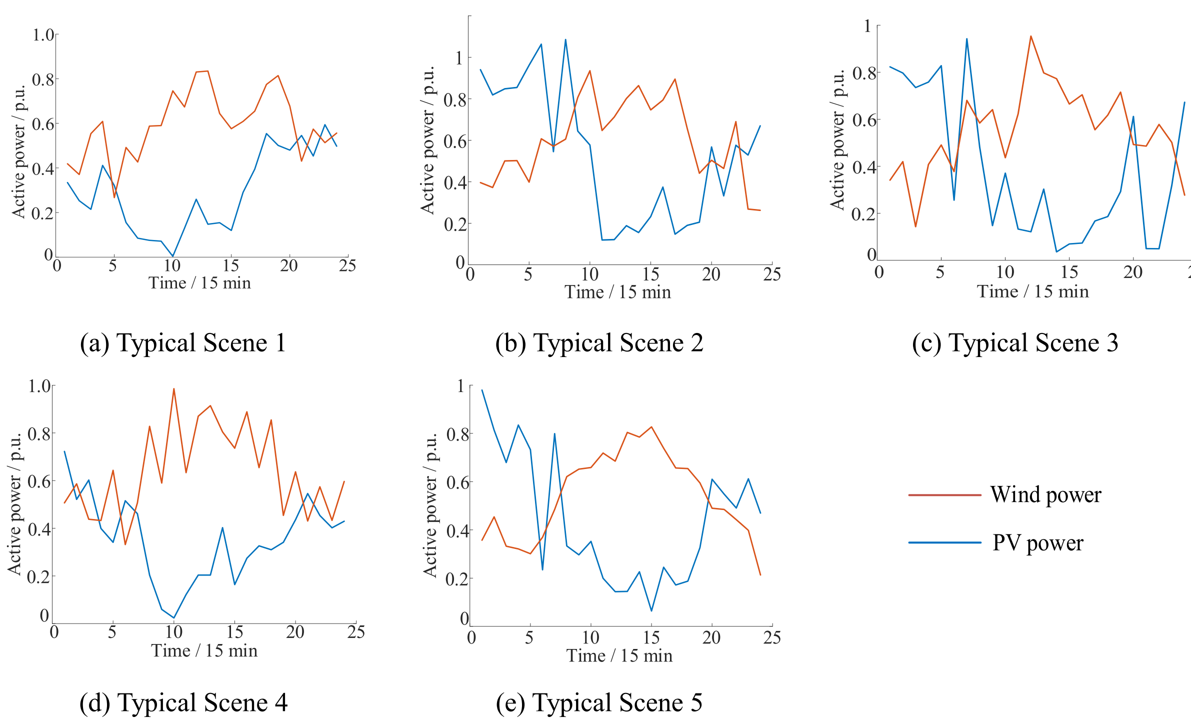

Fig. 5. Typical scenes of joint output of wind and PV power.

Table 1
Probability of occurrence of typical wind and PV power output.

Typical Scene	1	2	3	4	5
Probability of Occurrence	0.05	0.23	0.025	0.405	0.29

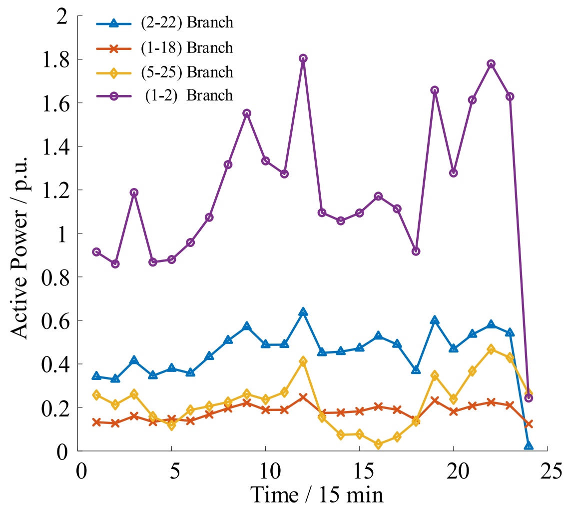

Fig. 6. Active power loss due to lightning-caused trip out.

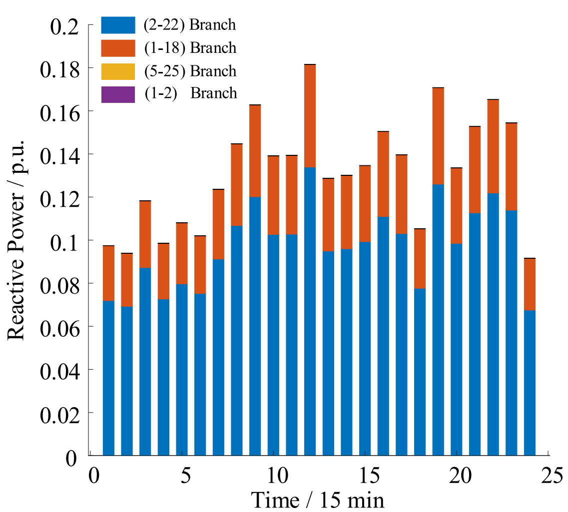

Fig. 7. Reactive power loss due to lightning-caused trip out.

$$\begin{cases} P_{t,\min}^{TSL} \leq P_t^{TSL} \leq P_{t,\max}^{TSL} \\ \sum_{i=1}^{T} P_t^{TSL} = 0 \end{cases}, \tag{42}$$

where P_t^{TSL} is the power of the load with time shift at time t. $P_{t,\max}^{TSL}$ and $P_{t,\min}^{TSL}$ are the upper and lower limit of the time shift power at time t.

The interruptible characteristics represent the power of the load can be cut down within the accepted range, so that when the power supply is short, part of the loads can be cut off to relieve the pressure and keep the stability of the operation. Corresponding constraints can be described as

$$0 \leq P_t^{IL} \leq P_{t,\max}^{IL}, \tag{43}$$

where $P_{t,\max}^{IL}$ is the maximum interruptible power of the load at time t.

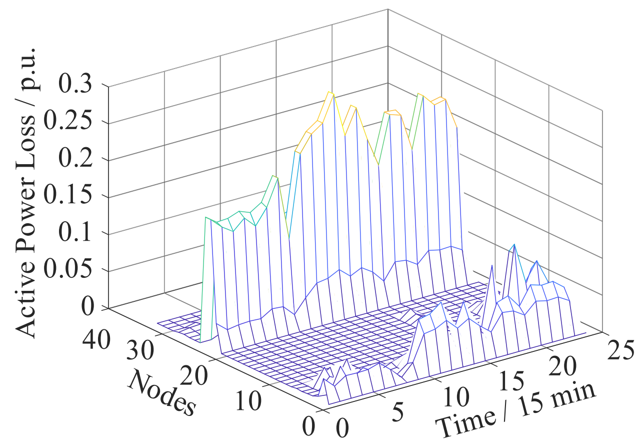

Fig. 8. The expected active load loss due to the accident between Node 1 and Node 2.

4. Simulation

4.1. Risk estimation

The IEEE 33 nodes power distribution system, as shown in Fig. 3, is used in this chapter as the simulation example. In this model, the reference value of apparent power and voltage is 1 MW and 12.66 kV, respectively. The testing system contains an array of PV cells, a wind turbine, 2 sets of power storage battery, and 3 SVC devices, whose configures are as follows:

PV cells: rated power 600 kW, connected on Node 32.
Wind turbine: rated power 1000 kW, rated wind speed 12 m/s, connected on Node 17.
Power storage battery: ESS1: maximum power 400 kW, minimum state of charge (SOC) 0.18, connected on Node 15. ESS2: maximum power 300 kW, minimum SOC 0.1, connected on Node 23.
SVC: maximum output reactive power 500 kvar, maximum absorbing reactive power 100 kvar. Define positive value as output, and negative value as absorbing.
The testing system is connected to the higher-level grid through Node 33.

In this chapter, the power fluctuation of the loads in the network is not under consideration, and the initial load data is introduced as the accurate predicted value, as shown in Fig. 4.

4.1.1. Generation of the typical wind and PV power output scenes

The historical data of the wind and PV output somewhere is selected as the samples for simulation. Each data sample is of 6 h long with 15 minutes' interval. 200 samples are selected in this procedure, and 5 typical scenes are obtained after cutting down, as shown in Fig. 5, and the probability of occurrence is displayed in Table 1.

4.1.2. Analysis of the lightning-caused load loss

In this chapter, an assumption is made that each distribution line in IEEE 33-node system has the same probability to be stroke by lightning. However, the load loss and operation risk of being stroke differs from each other due to the different topological position and load. In conventional distribution systems, the shorter the distance between the stroke point and the power source, the large the load loss will be. Nevertheless, such regulations are inapplicable in distribution systems with distributed power sources, and the weak point of the system should be reappraised.

In IEEE 33-node system, the branches between Node 2 and Node 22, Node 1 and Node 18, Node 5 and Node 25, and Node 1 and Node 2 are

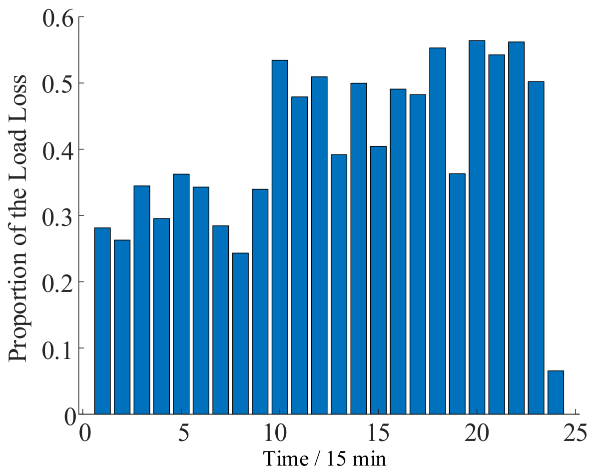

Fig. 9. The proportion of the load loss due to the accident between Node 1 and Node 2.

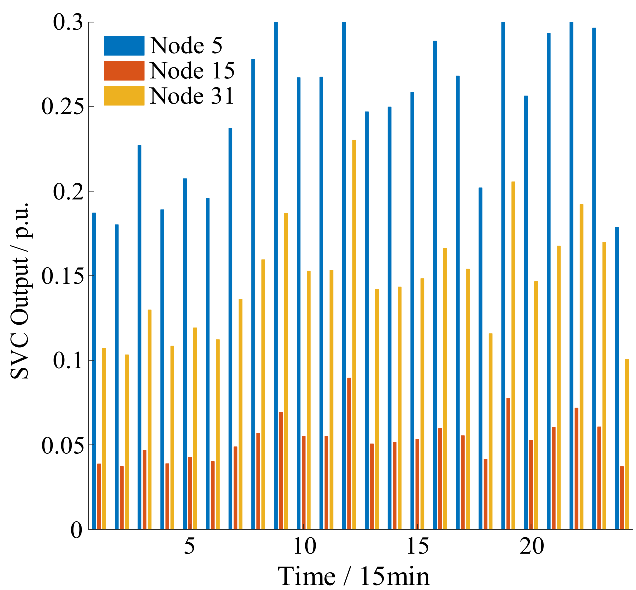

Fig. 10. SVC output after the trip out of the branch between Node 1 and 2.

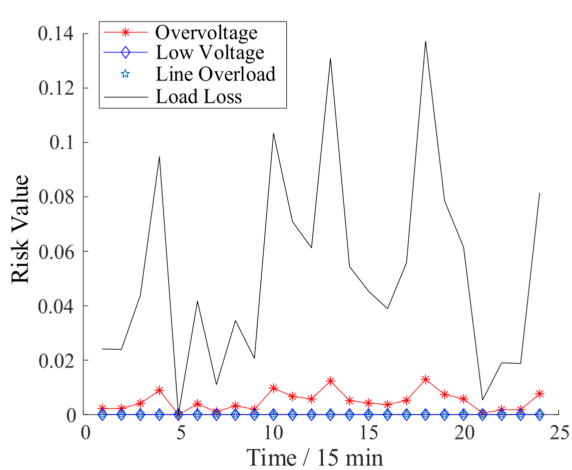

Fig. 11. The operation risk of the distribution network during estimation period.

the major branches which will result in the most severe load loss if tripped out by lightning strikes. Hence, faults on the above 4 branches will be simulated in order to find the weak point of the system. The active and reactive load loss caused by the 4 types of accidents are illustrated in Fig. 6 and Fig. 7, respectively. It can be found that the active power loss of the trip out of the branch between Node 1 and Node 2 is much larger than the other branches. However, the corresponding reactive power loss is closed to zero, which means this branch is the weakest point of active load in the system, and meanwhile, due to the existence of the SVC devices, the reactive load is not impacted. Consequently, such accident requires more active power source, and no more reactive power source is needed.

In order to reflect the influence of lightning-caused trip out to each node, the trip-out accident of branch between Node 1 and Node 2 is taken as an example to calculate the expected load loss and the risk level. Is the expected active load loss due to the accident between Node 1 and Node 2, and is the proportion of load loss of the whole distribution network caused by the accident. It can be found that although the proportion of load loss is high in this situation, the load loss between Node 14 and Node 21 is closed to zero. Because of the distributed power source, the power supply on the branch between Node 14 and Node 17 is not interrupted. However, due to the long length of the branch, the power of the source is not high enough to supply the whole branch, which results in the load loss on the other nodes. Besides, due to the power supply from the wind turbine, loads on Node 31 and 32 are not interrupted either.

Fig. 10 illustrates the reactive power output of the SVC devices after the trip out accident. As the accident makes the distribution system lose the reactive power supply from the higher-level grid, the output of the SVC devices becomes higher to satisfy the power requirement and reduce the network loss.

Based on the simulation results, it can be found that the average proportion of load loss when the accident between Node 1 and 2 occurred exceeds 30%, and preventive control measures should be done against such situation. Similar procedure can be done to calculate the load loss due to the trip out of different branches, and corresponding preventive adjustment can be planned.

4.1.3. Estimation of the risk caused by the indeterminacy of wind and PV output in lightning weather

In order to take full advantage of the wind and solar power, normally the wind turbine and PV batteries will be fully used. Due to the forecast error of wind and illumination in lightning weather, overvoltage and power flow off-limit may occur in the distribution system, and bring operation risk to the network. In this chapter, the extreme case which the SVC and ESS devices do not take part in the control procedure will be considered, in order to estimate the maximum risk caused by the indeterminacy of wind and PV output.

(1) Analysis of time series risk

Fig. 11 indicates there is little risk about low voltage or line overload in the system, and the major risk is consisted of load loss and overvoltage. During the whole estimation period, the load loss risk is high, and because of the high output of wind turbines, the reactive power cannot be effectively absorbed, which results in the overvoltage on the nodes.

Fig. 12 illustrates the risk of voltage off-line of the nodes in the distribution system. The overvoltage risk of Node 17 and Node 32 is shown in Fig. 12(c). Since the two nodes are the access points of distribution generation (DG), it is more probable for the overvoltage to occur on these two nodes, especially on Node 17, as the wind turbine usually has higher output than the PV arrays in lightning weather.

(2) Prewarning of the accident

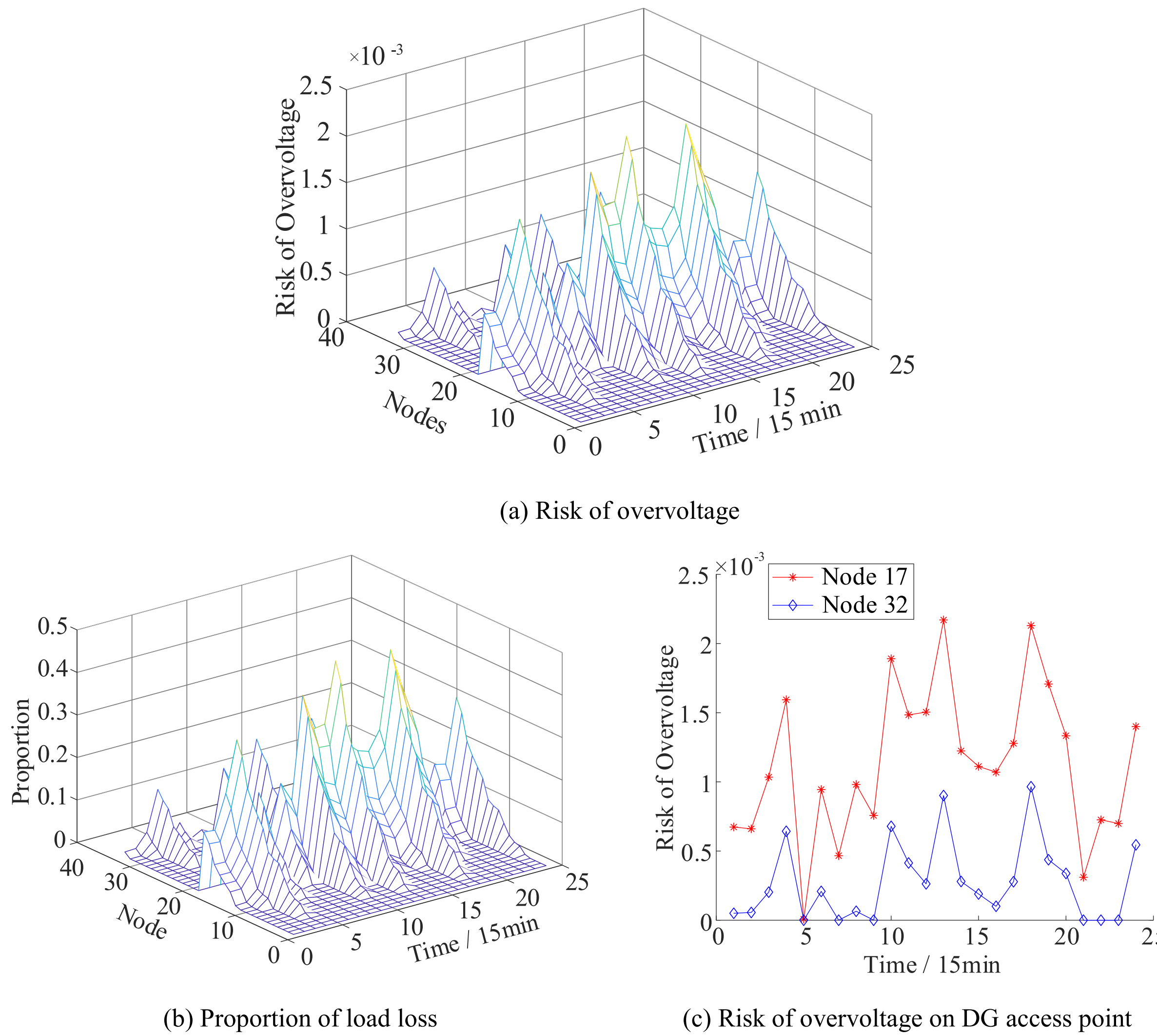

Fig. 12. Risk of voltage off-limit in the estimation period.

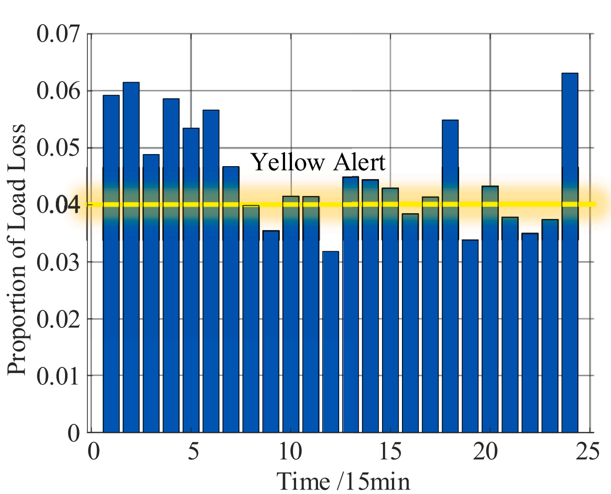

Fig. 13. Proportion of load loss in the estimation period.

Fig. 13 is the proportion of load lost in the estimation period of the distribution system [13]. Obviously, at most of the time, the proportion of load loss is more than 4%, which is set as the yellow alert level in the distribution system, and actions should be taken to keep the power supply for the loads.

Fig. 14 is the predicted risk of the network in the 18th time interval, and considering the expected load loss on branch between Node 1 and Node 2, red alert may be announced at the time.

4.2. Loss prevention

As the risk of the network has been predicted, topological reconstruction could be done to reduce the upcoming load loss in lightning weather. Since only the branch between Node 1 and 2 is threatened by lightning, reconstruction should be done for only once to reduce the introduced instability. According to the proportion of load loss illustrated in Fig. 9, the largest load loss occurred in the 20th time interval, so the preventive reconstruction should be done based on the power of the load at that time, and the topology of the system after reconstruction is shown in Fig. 15. Once the branch between Node 1 and 2, the load on the branch can be transferred to the branch between Node 1 and 18, and the stability of power supply can be enhanced.

Due to the access of the distributed generation, the voltage of the network after reconstruction may also be off-limit, so optimization

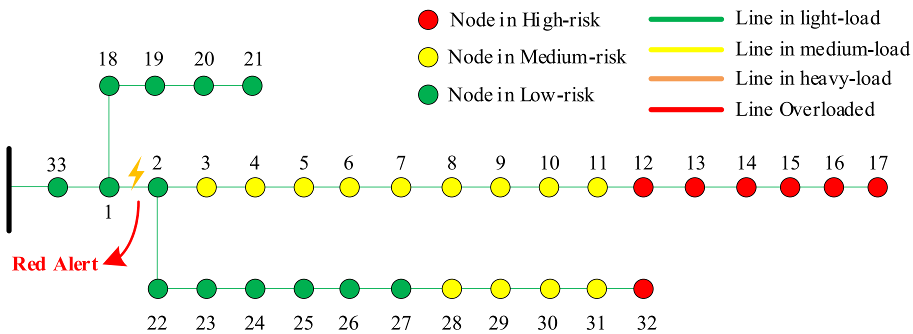

Fig. 14. The predicted risk of the nodes and lines in the distribution system in the 18th time interval.

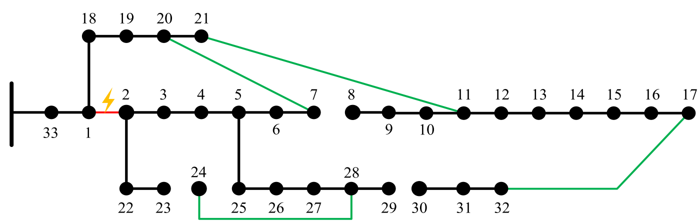

Fig. 15. Topology of the distribution system after reconstruction.

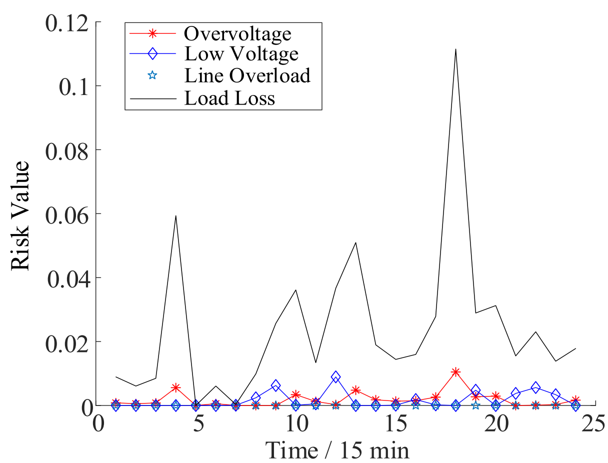

Fig. 16. The operation risk of the distribution network after reconstruction.

should be done for stable operation. Fig. 16 illustrates the operation risk of the distribution network after construction while energy storage, the SVC adjustment and the wind and PV power abandonment is not considered in such situation [14].

Obviously, risk about overvoltage [15], low voltage and load loss is existed in the distribution system after reconstruction. The fluctuation of the output of PV and wind power leads to the fluctuation of the risk value, especially when the output of the wind power increase, the reactive power cannot be effectively absorbed by the system, and results in the overvoltage. Besides, some branches are so long that low voltage may occur on some of the nodes far away from the power source, and meanwhile enhance the risk of load loss. Hence, it is necessary to optimize the resource in the system, to ensure the stable operation and the power supply of the load. The results of the optimization are shown in Fig. 17, and the voltage of the system after optimization is shown in Fig. 17(f).

Compare the node voltage before and after optimization in the 4th, 10th, 13th, and 18th time interval with the highest risk of overvoltage, and the results are shown in Fig. 18. It can be found that the optimization steps effectively reduced the voltage excursion, and improved the resilience to the risk of overvoltage caused by the indeterminacy of the wind and PV power output. The measures used in the optimization, including the reduction of PV and wind power output, and the adjustment of ESS and SVC power, can help to improve the stability of distribution system operation, and cut down the probable load loss in extreme weather [16].

5. Conclusion

The lightning problem has attracted much attention from the researchers of the power industry due to the climate change in recent years, and the DLP strategy for lightning protection in power systems has begun to be accepted by the public. In this manuscript, lightning protection issues for distribution networks are focused, and risk estimation model and preventive protection method are proposed to reduce the damage to the distribution system from the lightning weather.

Due to the fast development of distributed generations [17], more controllable resource is introduced into the distribution network, along with more indeterminacy caused by the output fluctuation of wind and PV power. In order to establish the lightning risk estimation model, the historical data of the wind and PV output are collected and analyzed to extract several presentive scenes of DP output, and the operation risk is analyzed considering not only the direct load loss caused by the lightning strikes, but also the indirect loss induced by the fluctuation of the DP output.

Based on the risk estimation, corresponding preventive protection could be carried out in two stages, namely the power flow transferring by topological reconstruction, and the coordination of the controllable resource such as the adjustment of the ESS, SVC, and DP output.

Simulations are done on the IEEE 33-node system. The operation risk and probable load loss caused by the lightning strike is calculated using the estimation model, and corresponding preventive steps are taken on the network, along with the other controllable devices in the system. The results indicates that the topological reconstruction and the

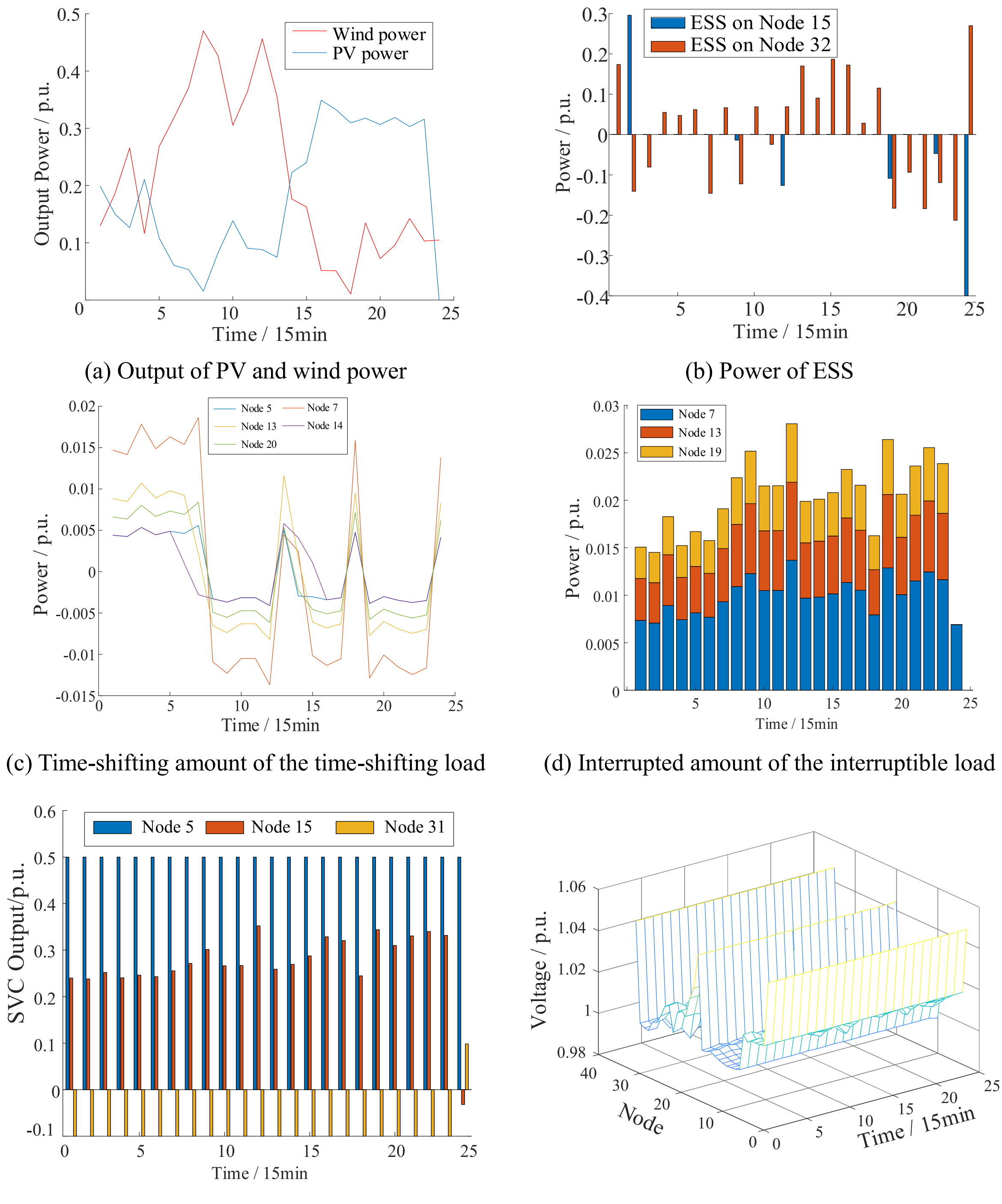

(a) Output of PV and wind power

(b) Power of ESS

(c) Time-shifting amount of the time-shifting load

(d) Interrupted amount of the interruptible load

(e) Reactive power of the SVC

(f) Voltage of the system

Fig. 17. Results of the optimization.

optimization to the distributed power source can help to improve the stability of distribution system operation, and cut down the probable load loss in extreme weather.

In the future, researches will be done on the transmission system to verify the feasibility of DLP application in power systems with long distance and high voltage level.

CRediT authorship contribution statement

Yang Xu: Conceptualization, Methodology, Writing – original draft, Writing – review & editing. **Chong Tong:** Conceptualization, Supervision, Project administration. **Min Xiang:** Data curation, Validation. **Tao Wang:** Software, Formal analysis, Validation. **Jian Xu:** Supervision, Writing – review & editing. **Jianyong Zheng:** Supervision.

Declaration of Competing Interest

The authors declare that they have no known competing financial interests or personal relationships that could have appeared to influence the work reported in this paper.

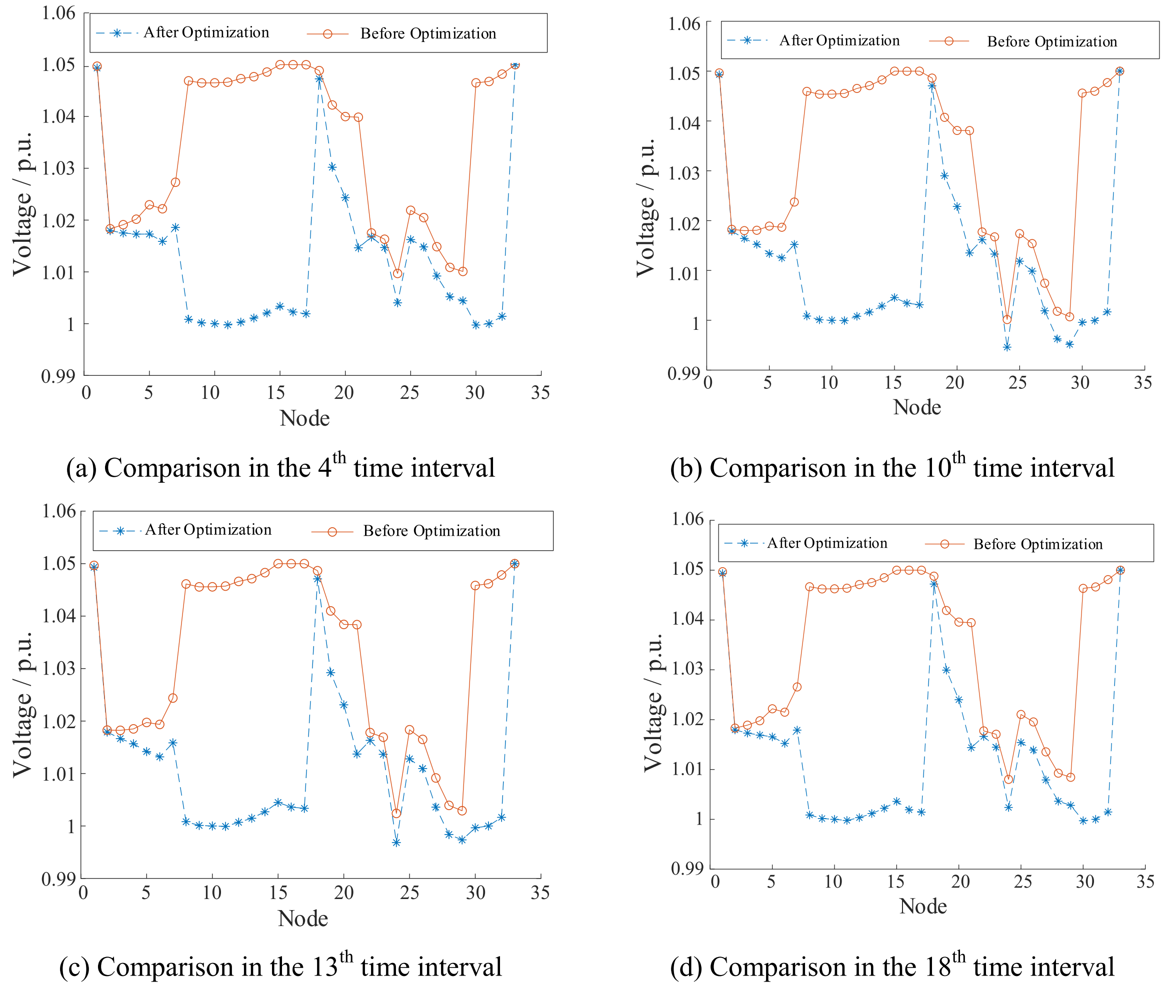

Fig. 18. Node voltage before and after optimization.

Data Availability

Data will be made available on request.

References

[1] A. Piantini, Lightning protection of overhead power distribution lines[C]//, in: 29th International Conference on Lightning Protection, Uppsala, Sweden, 2008, pp. 1–29.

[2] C. Tong, Q. Wang, Y. Gao, et al., Dynamic lightning protection of smart grid distribution system[J], Electr. Power Syst. Res. 113 (2014) 228–236.

[3] M. Xiang, Y. Xu, C. Tong, et al., A method of dynamic control of the power grid based on real-time lightning tracking[C]//, in: 35th International Conference on Lightning Protection (ICLP), IEEE, 2021.

[4] C. Tong, Y. Gao, Q. Wang, et al., Coordination of dynamic lightning protection and smart grids state estimation[C]//, in: 2014 International Conference on Lightning Protection (ICLP), IEEE, 2014, pp. 1027–1035.

[5] L. Feng, J. Zhang, G. Li, et al., Cost reduction of a hybrid energy storage system considering correlation between wind and PV power[J], Protect. Control Modern Power Syst. 1 (1) (2016) 1–9.

[6] H.V. Haghi, M.T. Bina, M.A. Golkar, et al., Using Copulas for analysis of large datasets in renewable distributed generation: PV and wind power integration in Iran[J], Renew. Energy 35 (9) (2010) 1991–2000.

[7] M. Liu, Wind power system risk assessment based on fuzzy clustering and copula function modeling[J], Energy Power Eng. 9 (04) (2017) 352.

[8] Y. Harmand, M. Trotignon, J.F. Lesigne, et al., Analysis of a voltage collapse-incident and proposal for a time-based hierarchical containment scheme[C]//, CIGRE Power Oper. Control (1990).

[9] W. Wu, K. Wang, B. Han, et al., A versatile probability model of photovoltaic generation using pair copula construction[J], IEEE Trans. Sustain. Energy 6 (4) (2015) 1337–1345.

[10] S. Hagspiel, A. Papaemannouil, M. Schmid, et al., Copula-based modeling of stochastic wind power in Europe and implications for the Swiss power grid[J], Appl. Energy 96 (2012) 33–44.

[11] N. Balijepalli, S.S. Venkata, C.W. Richter, et al., Distribution system reliability assessment due to lightning storms[J], IEEE Trans. Power Deliv. 20 (3) (2005) 2153–2159.

[12] G. Li, M. Peng, Dynamic reconstruction of active distribution network with electric vehicles[C]//, in: 2017 International Conference on Circuits, Devices and Systems (ICCDS), IEEE, 2017, pp. 127–130.

[13] D. Nie, L. Fan, K. Wang, et al., Research on AHP-based multi-factor medium voltage distribution network line risk quantitative assessment method[C]//, in: 2021 China International Conference on Electricity Distribution (CICED), IEEE, 2021, pp. 38–41.

[14] T.L. Sheu, Y.H Wang, Dynamic layer adjustments for SVC segments in P2P streaming networks[C]//, in: 2010 International Computer Symposium (ICS2010), IEEE, 2010, pp. 793–798.

[15] Z.H. Rather, B.C Pal, Voltage-dip induced frequency excursions in solar PV power integrated power system[C]//, in: 2020 IEEE International Conference on Power Systems Technology (POWERCON), IEEE, 2020, pp. 1–6.

[16] H. Ruan, H. Gao, Y. Liu, et al., Distributed voltage control in active distribution network considering renewable energy: a novel network partitioning method[J], IEEE Trans. Power Syst. 35 (6) (2020) 4220–4231.

[17] L. Jun, Study on loss allocation of power distribution network with distributed generation[C]//, in: The 2nd International Symposium on Power Electronics for Distributed Generation Systems, IEEE, 2010, pp. 678–680.